

Table S1. Entrapment efficiencies of pBAE nanoparticles encapsulating different types of nucleic acids (each type in a different color).

Nucleic acid type	MW, in Da(kb)	Entrapment efficiency (%)
Scrambled siRNA	12,000	66
GFP siRNA	13,300	71
mTOR siRNA	9,500	91
pMAX-GFP plasmid	129,500 (3.5kb)	92
Custom plasmid	444,000 (12 kb)	54
eGFP mRNA	36,000 (0.99 kb)	89
fLuc mRNA	71,410 (1.93 kb)	82
OVA mRNA	53,280 (1.44 kb)	77

This Table details some examples of nucleic acid entrapment efficiencies in pBAE nanoparticles, as a function of the nucleic acid and its length, as determined by the PicoGreen or RiboGreen colorimetric tests.

As clearly shown, in each group using the same type of nucleic acid, the entrapment efficiency increased when the molecular weight of the nucleic acid decreases. This was expected and is attributed to the use of the same polymer amount. We were maintaining the mass ratio between the polymer and the nucleic acid, thus, modifying N/P ratio (charges between cationic polymer and anionic nucleic acid), allowing more charges of polymer to encapsulate better the nucleic acid.

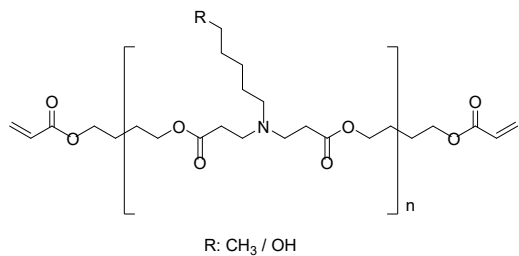


Figure S1. $^1\text{H-NMR}$ spectrum of C6 polymer.

$^1\text{H-NMR}$ (400MHz, Methanol- d_4 , TMS) (ppm): $\delta = 6.40$ (d, $\text{CH}_2=\text{CH}-$), 6.10 (d, $\text{CH}_2=\text{CH}-$), 5.83 (d, $\text{CH}_2=\text{CH}-$), 4.18 (br, $\text{CH}_2-\text{O}-\text{C}(=\text{O})-\text{CH}=\text{CH}_2$), 4.09 (t, $-\text{CH}_2-\text{CH}_2-\text{O}-$), 3.62 (t, $\text{CH}_2-\text{CH}_2-\text{OH}$), 2.78 (br, $-\text{CH}_2-\text{CH}_2-\text{N}-$), 2.45 (br, $-\text{N}-\text{CH}_2-\text{CH}_2-\text{C}(=\text{O})-\text{O}$), $1.83 - 1.60$ (br, $-\text{O}-\text{CH}_2-\text{CH}_2-\text{CH}_2-\text{CH}_2-\text{O}$), $1.40 - 1.18$ (br, $-\text{CH}_2-\text{CH}_2-\text{CH}_2-\text{CH}_2-\text{OH}$, $\text{N}-(\text{CH}_2)_2-\text{CH}_2-(\text{CH}_2)_2-\text{OH}$), 0.88 (t, $\text{CH}_2-\text{CH}_2-\text{CH}_3$).

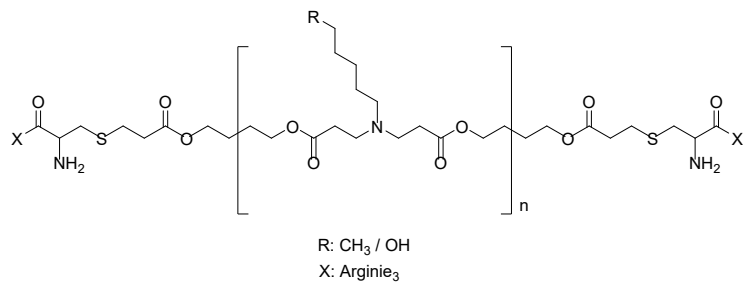


Figure S2. $^1\text{H-NMR}$ spectrum of C6-CRRR polymer.

$^1\text{H-NMR}$ (400MHz, Methanol- d_4 , TMS) (ppm): $\delta = 4.41 - 4.33$ (br, $\text{NH}_2-\text{C}(=\text{O})-\text{CH}-\text{NH}-\text{C}(=\text{O})-\text{CH}-\text{NH}-\text{C}(=\text{O})-\text{CH}-\text{CH}_2-$, 4.11 (t, $\text{CH}_2-\text{CH}_2-\text{O}$), 3.55 (t, $\text{CH}_2-\text{CH}_2-\text{OH}$), 3.22 (br, $\text{NH}_2-\text{C}(=\text{NH})-\text{NH}-\text{CH}_2-$, $\text{OH}-(\text{CH}_2)_4-\text{CH}_2-\text{N}-$), 3.04 (t, $\text{CH}_2-\text{CH}_2-\text{N}-$), 2.82 (dd, $-\text{CH}_2-\text{S}-\text{CH}_2$), 2.48 (br, $-\text{N}-\text{CH}_2-\text{CH}_2-\text{C}(=\text{O})-\text{O}$), 1.90 (m, $\text{NH}_2-\text{C}(=\text{NH})-\text{NH}-(\text{CH}_2)_2-\text{CH}_2-\text{CH}-$), 1.73 (br, $-\text{O}-\text{CH}_2-\text{CH}_2-\text{CH}_2-\text{CH}_2-\text{O}$), 1.69 (m, $\text{NH}_2-\text{C}(=\text{NH})-\text{NH}-\text{CH}_2-\text{CH}_2-\text{CH}_2-$), 1.56 (br, $-\text{CH}_2-\text{CH}_2-\text{CH}_2-\text{CH}_2-\text{OH}$), 1.39 (br, $-\text{N}-(\text{CH}_2)_2-\text{CH}_2-(\text{CH}_2)_2-\text{OH}$), 0.88 (t, $\text{CH}_2-\text{CH}_2-\text{CH}_3$).

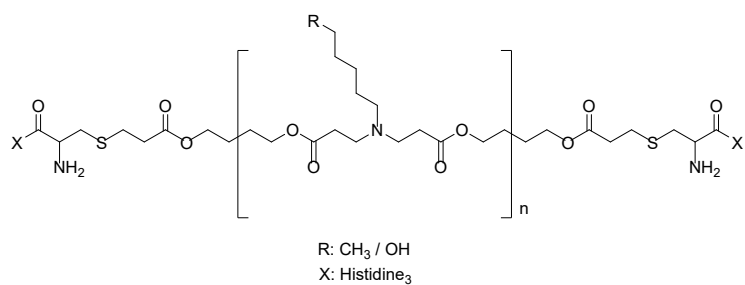


Figure S3. $^1\text{H-NMR}$ spectrum of C6-CHHH polymer.

$^1\text{H-NMR}$ (400MHz, Methanol- d_4 , TMS) (ppm): $\delta = 8.0 - 7.0$ (br, $-\text{N}=(\text{CH})-\text{NH}-\text{C}(=\text{CH})-$), $4.61 - 4.36$ (br, $-\text{CH}_2-\text{CH}-$), 4.16 (t, $\text{CH}_2-\text{CH}_2-\text{O}-$), 3.55 (t, $\text{CH}_2-\text{CH}_2-\text{OH}$), 3.18 (t, $\text{CH}_2-\text{CH}_2-\text{N}-$), 3.06 (dd, $-\text{CH}_2-\text{CH}-$), 2.88 (br, $\text{OH}-(\text{CH}_2)_4-\text{CH}_2-\text{N}-$), 2.82 (dd, $-\text{CH}_2-\text{S}-\text{CH}_2-$), 2.72 (br, $-\text{N}-\text{CH}_2-\text{CH}_2-\text{C}(=\text{O})-\text{O}$), 1.75 (br, $-\text{O}-\text{CH}_2-\text{CH}_2-\text{CH}_2-\text{CH}_2-\text{O}$), 1.65 (m, $\text{NH}_2-\text{CH}_2-\text{CH}_2-(\text{CH}_2)_2-\text{CH}-$), 1.58 (br, $-\text{CH}_2-\text{CH}_2-\text{CH}_2-\text{CH}_2-\text{OH}$), 1.40 (br, $-\text{N}-(\text{CH}_2)_2-\text{CH}_2-(\text{CH}_2)_2-\text{OH}$), 0.88 (t, $\text{CH}_2-\text{CH}_2-\text{CH}_3$).

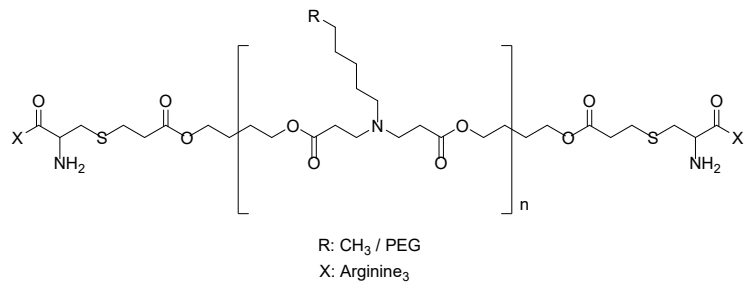


Figure S4. ¹H-NMR spectrum of C6-CRR-PEG polymer.

¹H-NMR(400MHz, Methanol-*d*₄, TMS) (ppm): δ = 4.41-4.33 (br, NH₂-C(=O)-CH-NH-C(=O)-CH-NHC(=O)-CH-NH-C(=O)-CH-CH₂-, 4.11 (t, CH₂-CH₂-O), 3.55 (t, CH₂-CH₂-OH), 3.22 (br, NH₂-C(=NH)-NH-CH₂-, OH-(CH₂)₄-CH₂-N-), 3.04 (t, CH₂-CH₂-N-), 2.82 (dd, -CH₂-S-CH₂), 2.48 (br, -N-CH₂-CH₂-C(=O)-O), 1.90 (m, NH₂-C(=NH)-NH-(CH₂)₂-CH₂-CH-), 1.73 (br, -O-CH₂-CH₂-CH₂-CH₂-O), 1.69 (m, NH₂-C(=NH)-NH-CH₂-CH₂-CH₂-), 1.56 (br, -CH₂-CH₂-CH₂-CH₂-OH), 1.39 (br, -N-(CH₂)₂-CH₂-(CH₂)₂-OH), 0.88 (t, CH₂-CH₂-CH₃).

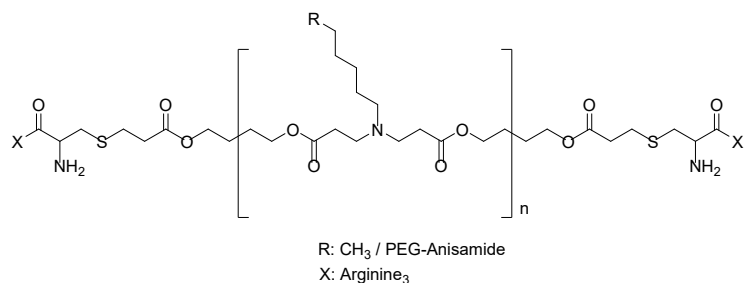


Figure S5. Chemical structure and ¹H-NMR interpretation of C6R-PEG-AA.

¹H-NMR(400MHz, Methanol-*d*₄, TMS) (ppm): δ = 4.41-4.33 (br, NH₂-C(=O)-CH-NH-C(=O)-CH-NHC(=O)-CH-NH-C(=O)-CH-CH₂-, 4.11 (t, CH₂-CH₂-O), 3.55 (t, CH₂-CH₂-OH), 3.22 (br, NH₂-C(=NH)-NH-CH₂-, OH-(CH₂)₄-CH₂-N-), 3.04 (t, CH₂-CH₂-N-), 2.82 (dd, -CH₂-S-CH₂), 2.48 (br, -N-CH₂-CH₂-C(=O)-O), 1.90 (m, NH₂-C(=NH)-NH-(CH₂)₂-CH₂-CH-), 1.73 (br, -O-CH₂-CH₂-CH₂-CH₂-O), 1.69 (m, NH₂-C(=NH)-NH-CH₂-CH₂-CH₂-), 1.56 (br, -CH₂-CH₂-CH₂-CH₂-OH), 1.39 (br, -N-(CH₂)₂-CH₂-(CH₂)₂-OH), 0.88 (t, CH₂-CH₂-CH₃).

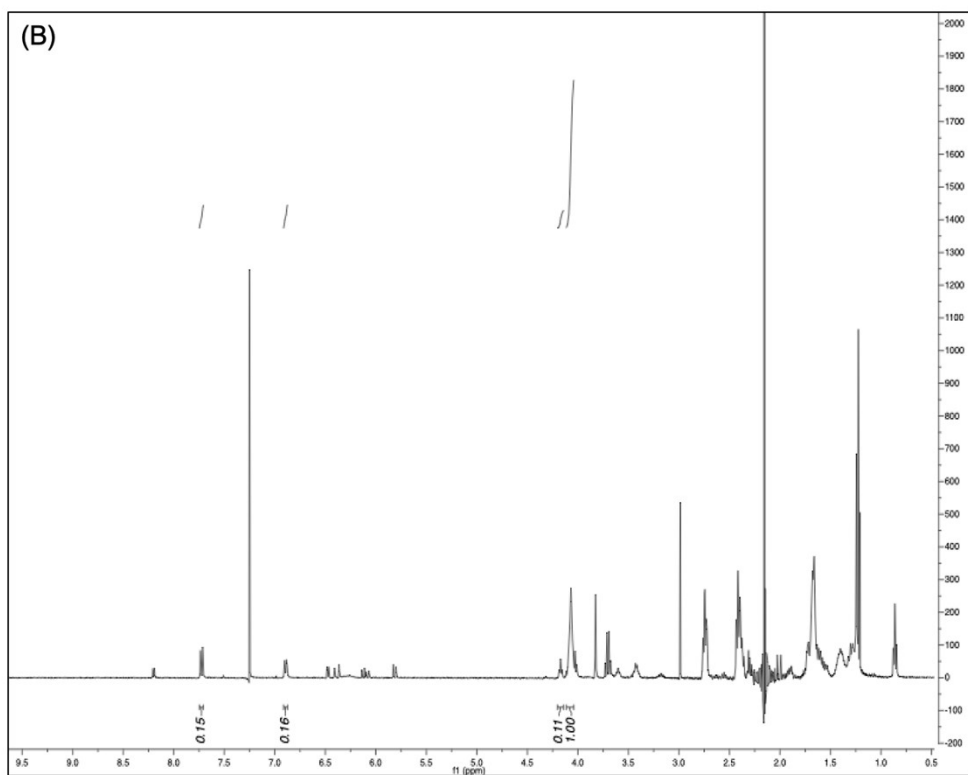
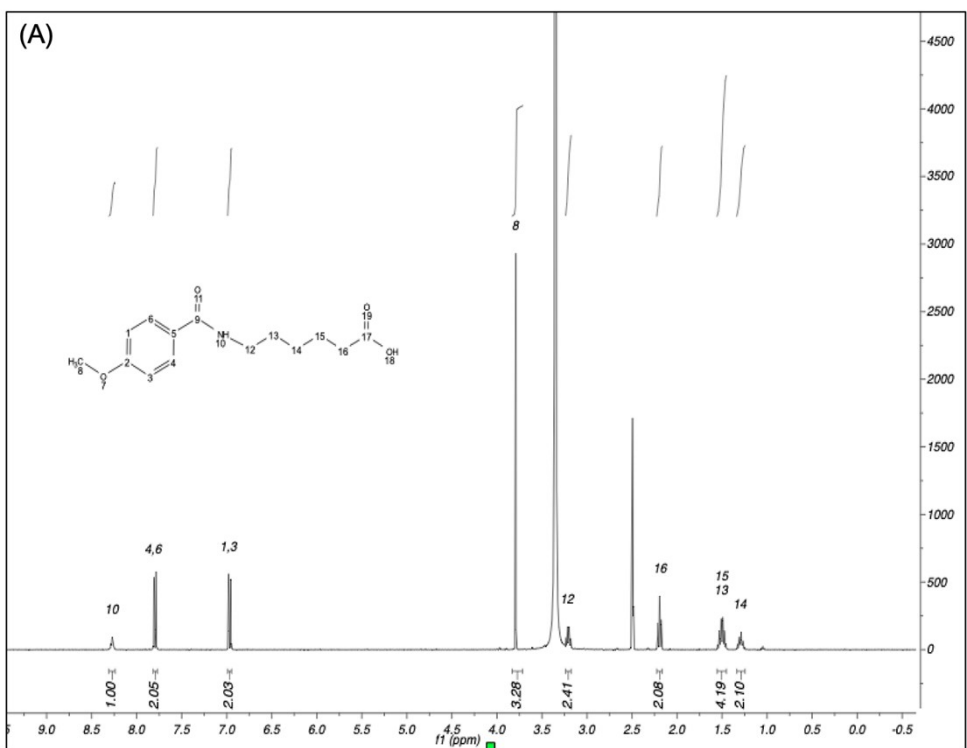


Figure S6. ¹H-NMR spectra of AA-pBAE. (A) NMR from the 6-(4-methoxybenzamido) hexanoic acid (AA). DMSO as solvent ($\delta = 2.53$ ppm). Peak at 3.47 ppm correspond to H₂O form the DMO. Peaks assignation, 8,7,2(3), 6(5) and 9 corresponding to the 4-methoxybenzoyl chloride and peaks 10,12,13,14,15 and 16 corresponding to the 6-aminocaproic acid. (B) NMR from the AA-pBAE conjugate. Chloroform-d ($\delta = 7.26$ ppm). Signal at $\delta = 2.16$ ppm corresponds to acetone (impurity form the MNR tube). Peaks assignation, between 1 and 4 ppm the peaks of pBAE and AA are mixed. Between 5.8 to 6.4 correspond to the acrylates of pBAE and from to 6.87 to 8.26 correspond to AA compound (protons form benzene and amide proton)

The presence of AA was confirmed by the peaks $\delta= 8.26$ ppm, $\delta= 7.79$ ppm and $\delta= 6.87$ ppm corresponding the first one to the amide and the other two to the protons of the benzene in para. Furthermore, it is possible to see the peaks corresponding to the olefins' signals associated to terminal acrylates of the pBAE at $\delta= 6.40$ ppm, $\delta= 6.10$ ppm and $\delta= 5.85$ ppm. The degree of esterification, the percentage of esterified pBAE out of total pBAE residues, was 33.3 % and was calculated dividing the peak corresponding to $\text{CH}_2\text{-O-C(=O)-CH=CH}_2$ ($\delta= 4.18$ ppm) and the peak corresponding to the protons of the benzene ($\delta= 6.87$ ppm) those ones that the integration is shown in the NMR, 0.1112 and 0.165 respectively.

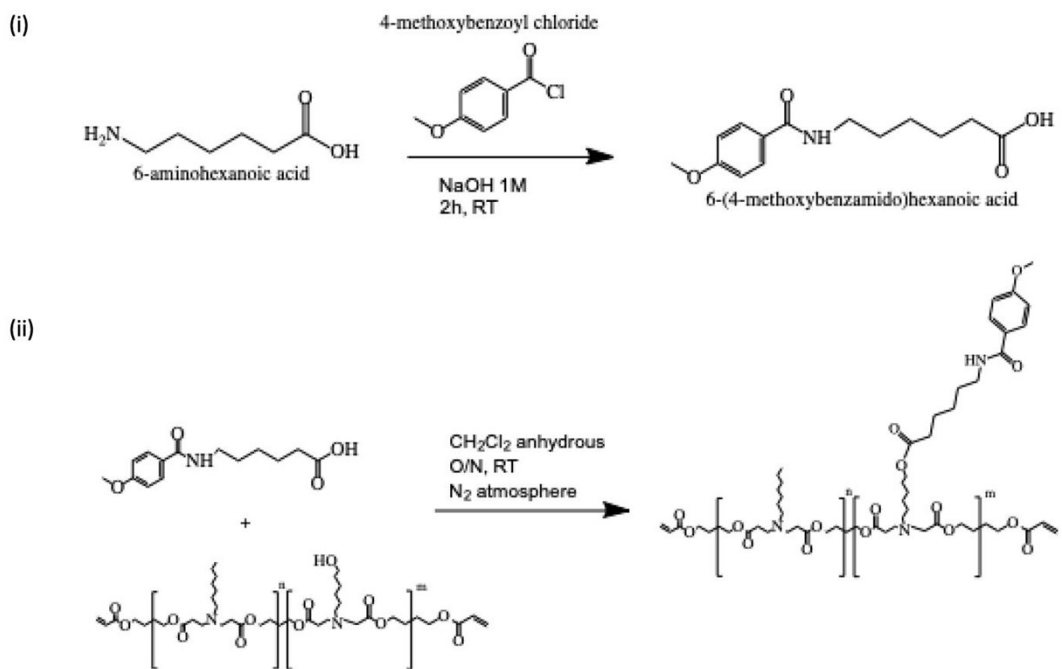


Figure S7. Synthesis of Anisamide conjugate polymer. (i) The AA conjugate was obtained by reaction between 6-aminocaproic acid and 4-methoxybenzoyl chloride. The reaction was done in NaOH 1M at room temperature for 2h (ii) The C6 polymer was esterified using the resulting product from the previous reaction, AA, with an esterification index of 50%. The reaction was carried out overnight at room temperature in CH₂Cl₂ anhydrous and in an atmosphere of N₂ (inert atmosphere).

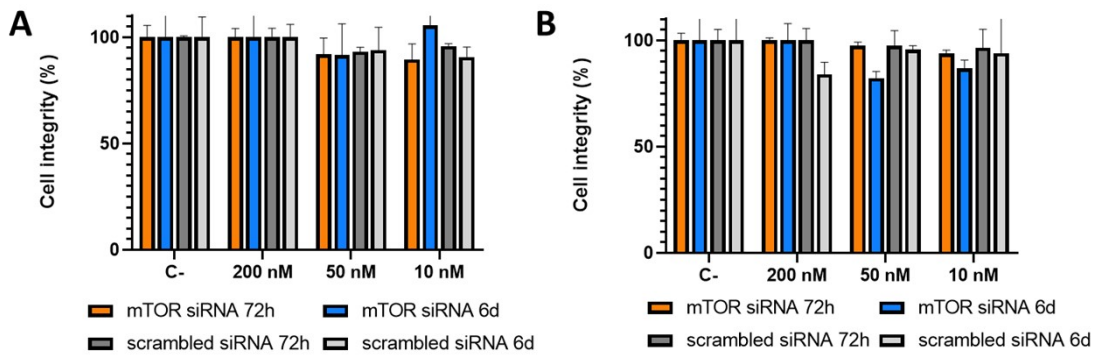
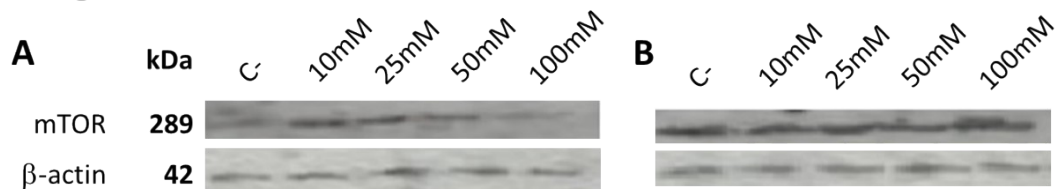


Figure S8: Viability of: A -A549 and B – BEAS-2B cells, after being incubated with OM-PBAE nanoparticles encapsulating siRNA, as a function of the encapsulated siRNA and time; using the LDH test to calculate the percentage of viability.

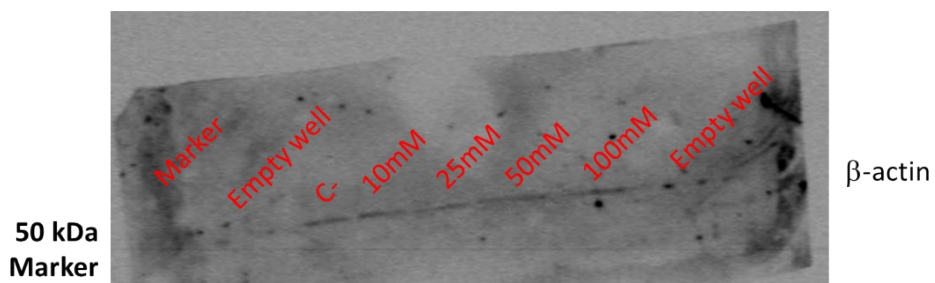
Lactate dehydrogenase test (LDH) measures the cell viability by assessing the activity of this enzyme, which can only be measured if released to cell culture media, that happens only when cell membrane is hampered and loses its integrity due to unspecific toxicity produced by some agents.

In our results, no changes in LDH test were observed for any of the samples tested, which confirms cell membranes integrity and thus, no unspecific toxicity was produced in these cases.

I. Figure 4A and 4B from the main text



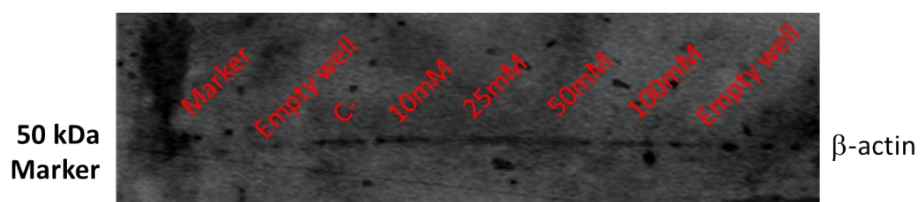
II. Gel corresponding to figure A, for the actin (lower half)



III. Gel corresponding to figure A, for the mTOR (upper half)



IV. Gel corresponding to figure B, for the actin (lower half)



V. Gel corresponding to figure B, for the mTOR (upper half)

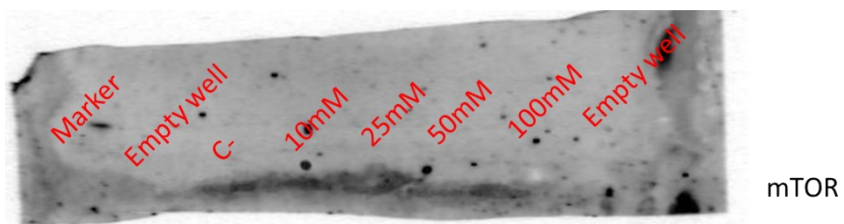


Figure S9: Complete western blot data, including processed blots (figure S9.I) and individual non-processed blots (figure S9.II to V).